PHYSICAL REVIEW B **93**, 064420 (2016)

Effect of Gd polarization on the large magnetocaloric effect of $GdCrO_4$ in a broad temperature range

E. Palacios,[1] C. Tomasi,[1,2] R. Sáez-Puche,[3] A. J. Dos santos-García,[4] F. Fernández-Martínez,[4] and R. Burriel[1]

[1]*Instituto de Ciencia de Materiales de Aragón (ICMA) and Departamento de Física de la Materia Condensada, CSIC–Universidad de Zaragoza, Pedro Cerbuna 12, 50009 Zaragoza, Spain*

[2]*IENI-CNR, Corso Promessi Sposi 29, 23900 Lecco, Italy*

[3]*Departamento Química Inorgánica, Facultad Químicas, Universidad Complutense Madrid, 28040 Madrid, Spain*

[4]*Departamento de Ingeniería Mecánica, Química y Diseño Industrial, ETSIDI, Universidad Politécnica de Madrid, 28012 Madrid, Spain*

(Received 12 November 2015; revised manuscript received 27 January 2016; published 19 February 2016)

The ferromagnetic zircon-type phase of $GdCrO_4$ presents high values for the magnetocaloric (MC) parameters. This compound has large isothermal entropy changes ΔS_T under the magnetic field action in a wide temperature range, from 5 to 35 K, reaching a maximum $|\Delta S_T| = 29.0 \pm 0.1$ J/kg K at 22 K, for a field increment $\Delta B = 9$ T. It orders ferromagnetically at $T_C = 21.3$ K via the Cr-Cr exchange interaction and shows a second transition at 4.8 K due to the ordering of the Gd sublattice. The large MC effect is enhanced by the polarization of the Gd^{3+} ions by the Cr^{5+} ones via a weaker Gd-Cr interaction. This effect is an interesting feature to be considered in the search for new compounds with a high MC effect in the range of liquid hydrogen or natural gas, regarding the liquefaction of gases by magnetization-demagnetization cycles. This paper contains experimental measurements of magnetization, heat capacity, and direct determinations of the MC effect. The magnetic contribution to the heat capacity C_m has been obtained after subtracting the lattice component. Approximate values for the exchange constants J_1 (Cr-Cr) and J_3 (Gd-Cr) have been deduced from C_m.

DOI: 10.1103/PhysRevB.93.064420

I. INTRODUCTION

The research on magnetocaloric materials has attracted worldwide interest in recent years due to their high potential use for magnetic refrigeration processes [1,2]. Gadolinium metal presents a magnetocaloric effect (MCE) through a second-order phase transition from paramagnetic (PM) to ferromagnetic (FM) at room temperature ($T_C = 293$ K), and it has been used as a cooling material in magnetic refrigeration prototypes since the 1970's, starting with the Brown refrigerator [3]. However, since 1997 when the so-called "giant MCE" was discovered by Pecharsky *et al.* in $Gd_5Si_2Ge_2$ [4], many studies have been done mainly in intermetallic compounds containing rare-earth elements [5]. In oxides, similar examples are abundant, especially for rare-earth transition metal oxides. $Gd_3Ga_5O_{12}$ (GGG) [6], $RMnO_3$ [7], RMn_2O_5 [8], and EuR_2O_4 [9], where R = rare earth, present high thermal and chemical stabilities and display large MCEs in the low-temperature region. New families without rare earths in their compositions have also been investigated as materials for refrigeration purposes close to room temperature [10].

Magnetic refrigeration is an alternative technology to traditional cooling systems based on cycles of compression and expansion of a gas. The efficiency can reach values up to 60% of a theoretical Carnot cycle and the absence of polluting gases constitutes a great advantage. It reduces expenses and improves profitability for liquefying fuel gases before transportation. Matsumoto *et al.* described a hydrogen liquefier based on the $Dy_3(Ga,Al)_5O_{12}$ garnet [11,12]. Therefore, magnetocaloric materials can be used as efficient refrigerants in the low-temperature range with the aim of producing the liquefaction of He, H_2, or natural gas [13].

It has been reported very recently that $RCrO_4$ (R = Ho, Gd, and Dy) oxides crystallizing with the zircon-type structure (space group $I4_1/amd$) show large values of the MC parameters [14,15]. Recently, we have succeeded in synthesizing $RCrO_4$ scheelite polymorphs (space group $I4_1/a$) by treating the zircon phases at high temperatures and high pressures [16].

The crystal structure, magnetic properties, and high pressure phase transformations of $RCrO_4$ zircon oxides have been previously reported [16–20]. Different mechanisms have been proposed to explain this first-order phase transition induced by pressure from zircon to scheelite and a reconstructive mechanism appears to account for it [21]. Reference [22] reports the MCE of a combination of these zircon phases with Gd and Er, derived from isothermal magnetization measurements. The coexistence of two magnetic ions, Cr^{5+} and R^{3+}, constitutes an interesting scenario to study $3d$-$4f$ magnetic interactions. Most of the zircon $RCrO_4$ oxides behave as ferromagnets, while the scheelite polymorphs are antiferromagnets. The change in the sign of the magnetic interaction can be explained considering the notable differences in the interatomic distances and Cr-O-R angles (see Fig. 1). Although the four- and eightfold coordinations remain in going from the zircon to the scheelite polymorph, there are some remarkable differences when these two structural types are compared. In the case of zircon, the structure can be described as formed by zigzag chains of edge-sharing RO_8 bisdisphenoids along the a axis of the tetragonal unit cell, connected to each other by sharing edges with CrO_4 tetrahedral units [Fig. 1(a)]. However, in the scheelite form, the CrO_4 tetrahedra are aligned along the a axis, while the RO_8 bisdisphenoids of different chains are forming dimers of R_2O_{14} composition and there is no edge sharing between RO_8 and CrO_4 polyhedra, as in the case of zircon [Fig. 1(b)]. Neutron diffraction studies reported that both rare-earth and chromium sublattices become ordered simultaneously at the same temperature [23] and the Cr^{5+} and R^{3+} ions will contribute to the MCE.

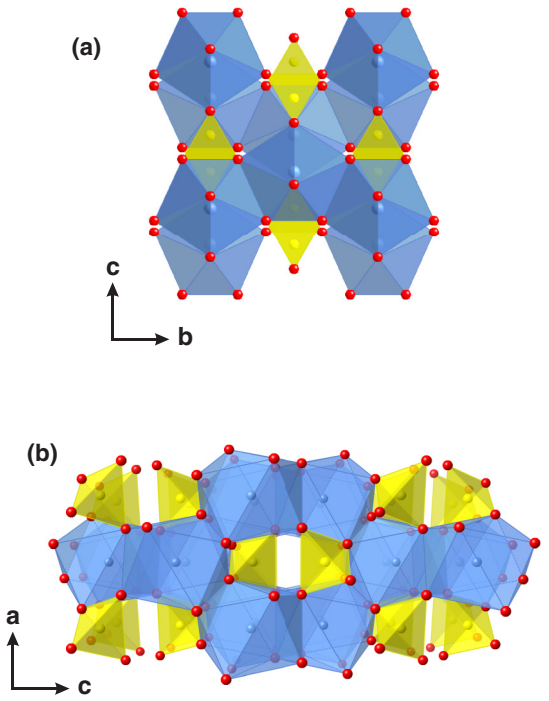

FIG. 1. Perspective view of the (a) zircon-type structure showing the zigzag chains of RO_8 bisdisphenoids (blue) along the a axis connected by edge-sharing CrO_4 tetrahedra (yellow) through the a axis. (b) RO_8 bisdisphenoids and CrO_4 tetrahedra sharing corners in the scheelite crystal structure.

In addition to the fundamental physical and chemical properties, the following features make these oxides suitable for potential refrigerants in comparison with other rare-earth transition metal oxides. First, a large magnetic moment, typical of many rare-earth ions, makes its polarization easier by a moderate external magnetic field. Second, a weak anisotropy and a weak crystal field favor the thermal population of all magnetic states (i.e., with a random distribution of the magnetic moment directions above T_N or T_C but still at low temperatures) at zero field. Third, the exchange interaction between $3d$ ions, usually much higher than the R-R exchange interaction, provides an internal field, increasing the polarization of the R ions below the ferromagnetic ordering temperature. The Cr^{5+} ion plays an important role as the promoter of the interactions in the rare-earth sublattice, increasing its ordering temperatures at least one order of magnitude in comparison with the analogous RXO_4 (X = P, As, V), where X is a diamagnetic element [24,25]. The case R = Gd is easier to analyze because, for this spin-only atom, the anisotropy and crystal-field energies are of the order of 1 K or less [24], therefore, a higher MCE is expected. Actually, $GdPO_4$ showed the strongest MCE ever observed with an isothermal entropy increment $-\Delta S_T = 62.1$ J/kg K at 2 K on application of a field of 7 T [24].

In this paper we report the magnetic and magnetocaloric properties of the zircon polymorph of $GdCrO_4$ oxide deduced from isothermal magnetization, heat capacity under field, and direct measurement of ΔS_T. The data have been analyzed assuming a stronger Cr-Cr ferromagnetic exchange interaction and a weaker Gd-Cr one. This Gd-Cr interaction is crucial to get a large MCE and gives a clue as to how to design materials for efficient magnetic refrigeration.

II. SAMPLE PREPARATION AND CHARACTERIZATION

The zircon-type $GdCrO_4$ powdered sample was prepared by heating stoichiometric amounts of $Gd(NO_3)_3 \cdot 6H_2O$ and $Cr(NO_3)_3 \cdot 9H_2O$ in an oxygen flow according to the following thermal process: 30 min at 433 K, 30 min at 473 K, and final treatment at 853 K for 12 h. Rietveld refinement of the x-ray diffraction data reveal that the Bragg reflections can be indexed according the tetragonal $I4_1/amd$ space group. A small amount of the secondary phase $GdCrO_3$ perovskite has been taken into account in the refinement.

The magnetization M has been measured in a standard Quantum Design superconducting quantum interference device (SQUID) magnetometer at several constant temperatures, from 4 to 40 K for fields between 0 and 9 T.

The heat capacity has been obtained by the conventional relaxation method in a Quantum Design physical properties measurement system (PPMS) setup. The calorimeter consists of a sapphire plate with a resistance thermometer and a heater. The sample is attached to the upper side of the plate. In addition to electrical connections, the wires supply mechanical support and a weak thermal contact to a bath at constant temperature T_0. For the determination of the heat capacity, a constant power is supplied to the heater. The relaxation time τ to the new equilibrium temperature gives the heat capacity C, knowing the sample mass m and the thermal conductance of the wires k, since in a rough approximation $\tau = mC/k$. Nevertheless, more elaborated models are used to fit the relaxation, including the finite thermal conductivity of the sample.

For the direct measurement of ΔS_T, a magnetic field is applied at a typical rate of 0.01 T/s while the temperature is recorded. During the field increase period the sample temperature T is above T_0, but relaxes again to thermal equilibrium with the bath when the field stabilizes at the final value. Knowing k, the entropy increment from the initial field B_1 at t_1 to the final value B_2 at t_2 is given by

$$\Delta S_{T_0} = S(B_2,T_0) - S(B_1,T_0) = \int_{t_1}^{t_2} \frac{k(T)(T_0 - T)dt}{T}. \quad (1)$$

Details of this procedure will be given elsewhere.

III. ISOTHERMAL MAGNETIZATION

The experimental magnetization as a function of field from 0 to 9 T, measured every 4 K between 4 and 40 K, have been plotted in Fig. 2(a). To clarify the discussion, the experimental $M_T(B)$ data have been plotted as functions of T at constant fields [Fig. 2(b)] in units of Bohr magnetons per formula unit containing one Gd and one Cr atom. This compound does not have thermal hysteresis, so the isothermal procedure used in the experiment saves measuring time and does not introduce substantial differences with respect to true isofield measurements.

The magnetization curves are consistent with the reported data of $M_T(B)$ [23] and with the heat capacity $C_{p,B}$ (Sec. IV B) that show a ferromagnetic transition with a Curie temperature $T_C = 21.3$ K, but present some unusual features, different than

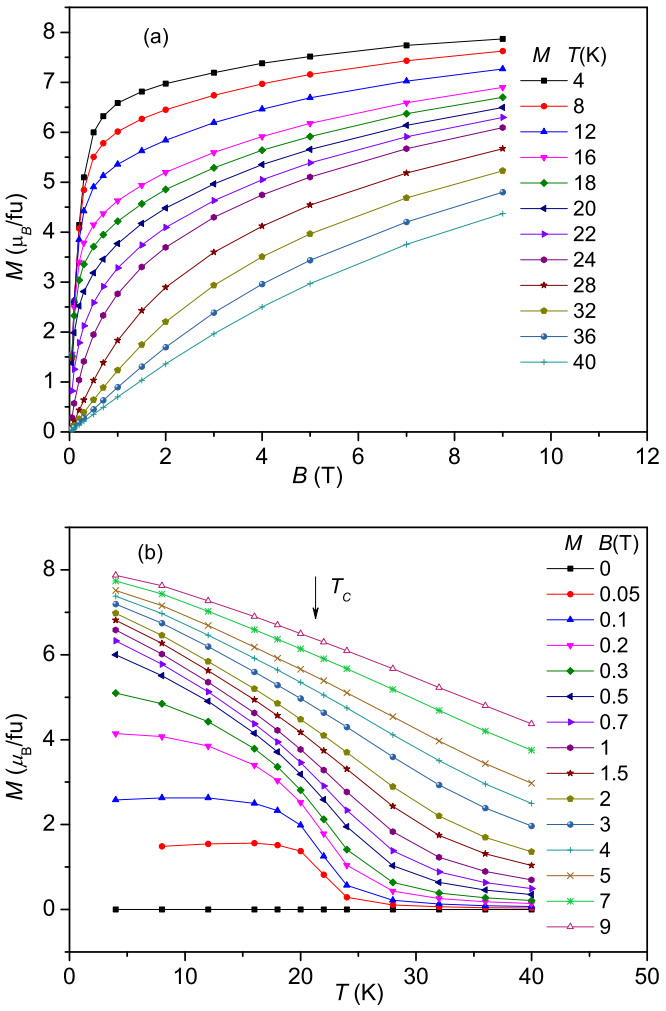

FIG. 2. (a) Field dependent magnetization measurements of $GdCrO_4$ from 0 to 9 T, between 4 and 40 K. (b) Representation of the temperature dependent magnetization obtained from the previous experimental $M_T(B)$ data.

in a typical ferromagnet. We leave out of the analysis the data at low fields, $B < 0.2$ T, where the sample shape affects the magnetization values through the internal demagnetizing field. For higher fields, M does not saturate quickly below T_C, but increases gradually on decreasing T, and the saturation is not reached even at 4 K, for fields as high as 9 T, where it reaches a value of $M = 7.87\mu_B$/f.u. The saturation magnetization M_s can be inferred to be $8\mu_B$/f.u., corresponding to the spin-only values for Gd^{3+} ($S = 7/2$) and Cr^{5+} ($S = 1/2$), in both cases with a gyromagnetic ratio $g = 2$. For Cr^{5+} this is clearly shown in cases where Gd is replaced by a nonmagnetic atom as in $YCrO_4$ [26]. For Gd^{3+} the spin-only value for the $4f^7$ electrons results in a magnetic moment of $7\mu_B$/atom. In other Gd compounds the saturation value is frequently higher than $7\mu_B$/atom due to the polarization of the conduction $6s$ or the $5d$ electrons, which in turn transfer the exchange via a Ruderman-Kittel-Kasuya-Yosida (RKKY) interaction. As an example, highly pure Gd metal has a saturation moment of $7.63\mu_B$/atom [27]. These electrons practically do not exist in $GdCrO_4$, that is electrically an insulator, with Gd^{3+} bonded ionically in a high percentage to the CrO_4^{3-} group. A very precise electron-paramagnetic resonance (EPR) determination of g in Gd^{3+}-doped zircon-type orthophosphates gave $g = 1.99$ [28]. These bonding characteristics produce a low Gd-Gd exchange interaction, crucial to have a high magnetocaloric effect at low temperatures (see Sec. V), as already observed in $GdPO_4$ [24].

In a usual ferromagnet, the magnetization increases below T_C and saturates rapidly. This is not the case for $GdCrO_4$, since at 15 K ($T = 0.7T_C$) and a field as high as 1 T, $M = 4.7\mu_B$/f.u., only slightly higher than $M_s/2$. Considering also the heat capacity and the magnetocaloric results, as discussed later, we interpret that the weak Gd-Cr exchange acts on the Gd sublattice polarizing the Gd^{3+} ions, but is not strong enough to orient them completely. This interaction would also act on the Cr sublattice raising T_C, which increases from 9.1 K for $YCrO_4$ to 21.3 K for $GdCrO_4$. This also explains the low moment at the Gd sublattice observed by Mössbauer spectroscopy just below T_C, at zero field [23].

IV. HEAT CAPACITY AND MAGNETOCALORIC EFFECT

A. MCE from magnetization

The isothermal entropy change as a function of temperature can be evaluated from magnetization measurements at different temperatures and magnetic fields by numerical integration of the well-known Maxwell relation

$$\left(\frac{\partial S}{\partial B}\right)_T = \left(\frac{\partial M}{\partial T}\right)_B \Rightarrow \Delta S_T = \int_0^{B_f} \left(\frac{\partial M}{\partial T}\right)_B dB. \quad (2)$$

Figure 2 shows the isothermal magnetization data as a function of the magnetic field up to 9 T at different temperatures above and below T_C. The magnetization curves confirm the ferromagnetic behavior below 22 K, and the value of the magnetic moment obtained below T_C indicates that both Gd^{3+} and Cr^{5+} ions contribute to the magnetic ordering. The isothermal entropy variation ΔS_T for different magnetic fields is shown in Fig. 3(a). A maximum is observed in the $-\Delta S_T$ values around 22 K, near the Curie temperature. $|\Delta S_T|$ decreases below T_C but not as quickly as expected for a ferromagnetic arrangement. Indeed, there is a bump near 10 K. The entropy change increases at T_C with increasing external field and reaches a value as high as 30 J/kg K for 9 T.

B. Heat capacity

Figure 4 shows the heat capacity of $GdCrO_4$ from 2 to 80 K. The peak at 21.3 ± 0.2 K can be ascribed to the ferromagnetic to paramagnetic transition at T_C observed in magnetization. The phonon contribution C_{ph} can be estimated from the heat-capacity values for another nonmagnetic zircon-type compound $C_0(T)$, applying a corresponding state law $C_{ph}(T) \simeq C_0(Tf)$, which is exact for the theoretical Einstein and Debye models and approximately valid for real solids when the scale factor f is close to unity. For this purpose, the fully diamagnetic compound $ZrSiO_4$ is not the best choice since $f = 1.6$ due to its much lighter atoms [29]. A more adequate compound is $LuCrO_4$ [26]. The Cr^{5+} ion introduces a magnetic component in its heat capacity, but this compound orders at $T_N = 9.1$ K and there is a wide T range above 20 K in which the magnetic contribution is negligible. Using

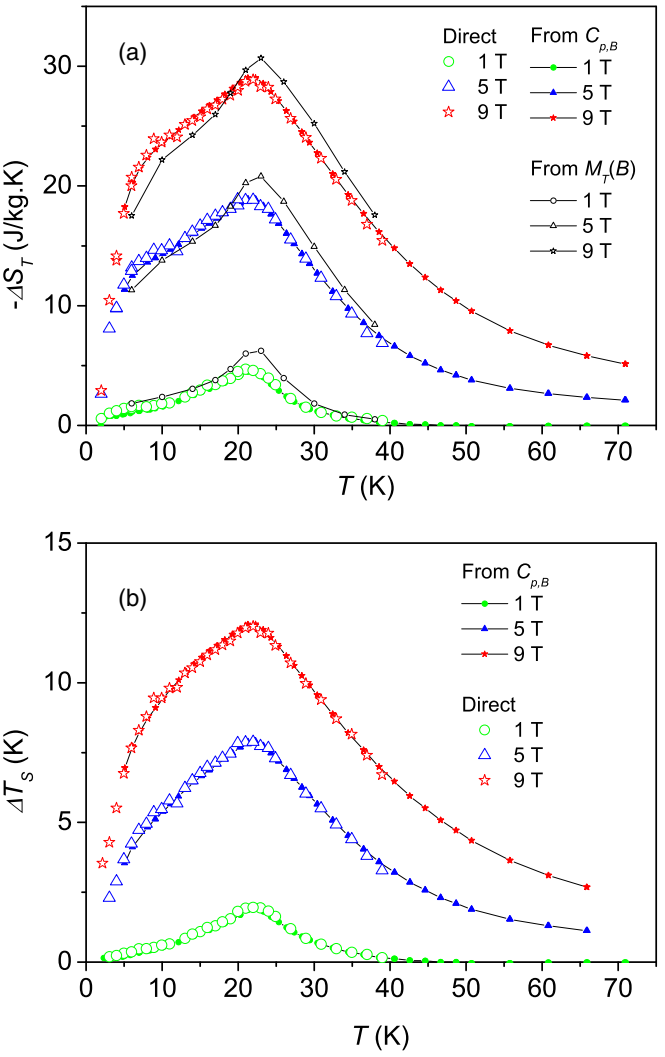

FIG. 3. Magnetocaloric parameters of $GdCrO_4$ for magnetic field changes from 0 to 1, 5, and 9 T: (a) Isothermal entropy change $-\Delta S_T$ obtained from $M_T(B)$, $C_{p,B}(T)$, and direct measurements. (b) Adiabatic temperature change ΔT_S.

$f = 1.07$, the C_p values for $LuCrO_4$ match quite well with the measurements for $GdCrO_4$ above 40 K, where their magnetic contributions are negligible.

Nevertheless, the Lu compound does not provide any phonon baseline below 20 K, due to its magnetic contribution. Then, we can make some theoretical considerations in order to determine C_{ph}. The zircon-type compounds have 18 phonon branches, but nine of them correspond to the internal modes of the CrO_4 tetrahedron, which have frequencies above 260 cm^{-1} (data for $YCrO_4$ from Raman spectroscopy) [30], giving Einstein temperatures above 370 K. These branches do not contribute appreciably up to 70 K. Among the nine remaining branches, three are acoustic and six are optical. C_{ph} can be fairly described by a three-dimensional Debye function (as in the case of one atom per formula unit) and a sixfold Einstein function. We took the data of $LuCrO_4$, affected by a scale factor, and fitted them to a sum of Einstein and Debye functions, resulting in their characteristic temperatures $T_E = 255$ K and $T_D = 155$ K, which matches the experimental

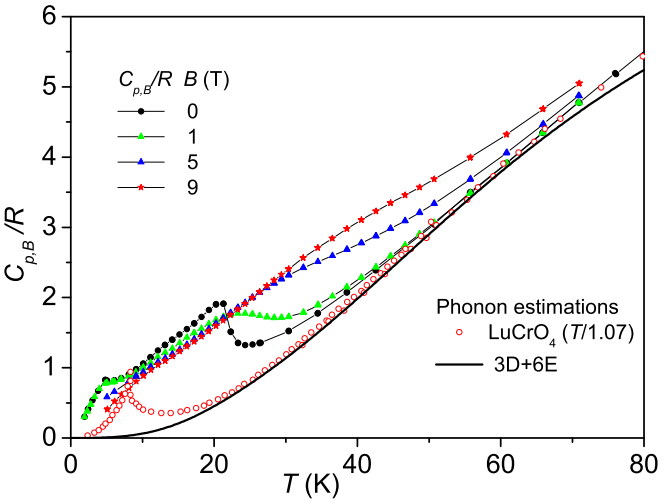

FIG. 4. Linked symbols: Heat capacity of $GdCrO_4$ for fields of 0, 1, 5, and 9 T. Open circles: Heat capacity of $LuCrO_4$, with T affected by a scale factor $f = 1.07$, used to determine the phonon contribution. Black line: Theoretical estimation of the baseline with a three-dimensional Debye function plus a sixfold Einstein function.

data between 20 and 60 K (Fig. 4), providing a physically reasonable baseline for $GdCrO_4$ as the phonon contribution.

To determine the absolute entropies at different fields, we have followed a procedure similar to the case used with $GdPO_4$ [24], using the direct measurements of ΔS_T for several fields. The heat-capacity measurements at $B = 0$ can be hardly extrapolated to $T \to 0$ due to the existence of a peak at 4.8 K, but the results for 9 T are smooth and can be extrapolated with an approximate $C_{p,9\,\mathrm{T}} = AT^{1.2}$ dependence. In any case, the entropy is small for 9 T at these low temperatures and any estimation errors are even smaller. Plotting the entropy for 9 T, the data extrapolate correctly to zero for $T \to 0$, giving $S(5.1\ \mathrm{K}, 9\ \mathrm{T})/R = 0.34$. For higher temperatures, the absolute entropy can be obtained by integration of $C_{p,9\,\mathrm{T}}/T$. For other fields, the directly measured ΔS_T with respect to 9 T at a single fixed temperature provides a proper integration constant, as explained in Sec. IV C.

With this estimation for the phonon part we find at 60.8 K the phonon entropy to be $S_{ph}/R = 2.10$, while the total entropy is $S/R = 4.89$ at zero field, giving a magnetic contribution $S_m/R = 2.79$, very close to the theoretical value for the spins 1/2 (Cr^{5+}) and 7/2 (Gd^{3+}), $S_{m,\mathrm{th}}/R = \ln 2 + \ln 8 = 2.77$.

The resulting "experimental" magnetic heat capacity $C_{m,B}(T) = C_{p,B}(T) - C_{ph}(T)$ is plotted in Fig. 5.

The comparison with other $RCrO_4$ compounds, where R = nonmagnetic atom, can give an idea about the Cr-Cr exchange interactions. The Cr ions form a distorted diamond lattice [26] in which each Cr ion has four nearest neighbors. $LuCrO_4$ orders antiferromagnetically at $T_N = 9.1$ K while $YCrO_4$, with very similar Cr-Cr distances and O-Cr-O angles, orders at 9.2 K, but ferromagnetically [26]. This different behavior is probably due to the competition of the exchange interactions between nearest and next-nearest neighbors, whose distance is not much higher. Isostructural compounds of $GdCrO_4$ in which Cr has been replaced by a nonmagnetic

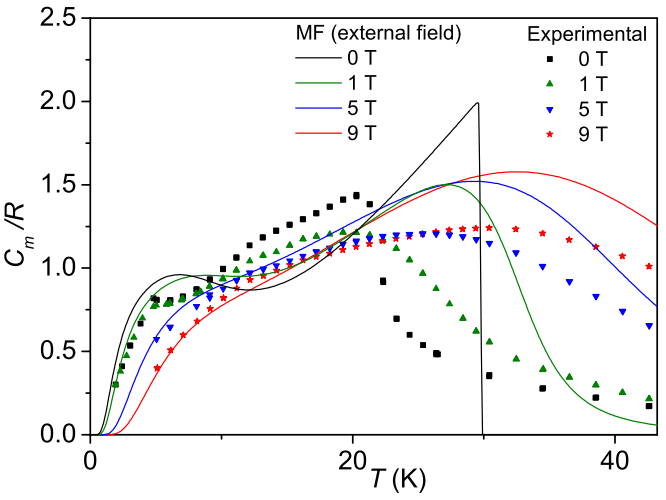

FIG. 5. Symbols: Magnetic heat capacity $C_{m,B}(T)$ of $GdCrO_4$ for fields of 0, 1, 5, and 9 T. Continuous lines: Mean-field calculations for $J_1/k_B = 25$ K, $J_2/k_B = 0$, $J_3/k_B = 10$ K.

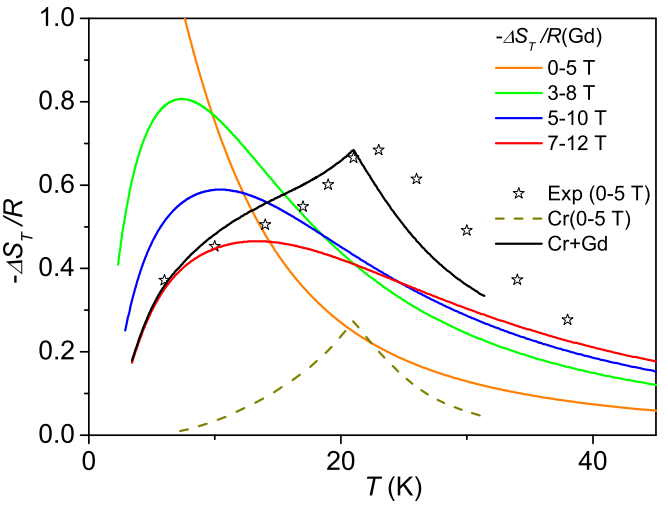

FIG. 6. Colored lines: $-\Delta S_T$ computed for a solid of paramagnetic atoms with spin 7/2 (Gd^{3+}) for the same field variation of 5 T, but with different initial fields (0, 3, 5, and 7 T). Dashed line: $-\Delta S_T$ for a ferromagnetic set of atoms with spin 1/2 (Cr^{5+}) and $T_C = 21$ K, computed via the mean-field theory of Bean-Rodbell with $\eta = 0.1$. Black line: Sum of the contributions of Cr and Gd for an initial field of 7 T. Symbols: Experimental results.

atom provide information about the Gd-Gd interaction. Gd also has four nearest neighbors. $GdVO_4$ and $GdAsO_4$ order antiferromagnetically at $T_N = 2.5$ and 1.26 K, respectively [31]. In all cases the behavior departs significantly from the mean-field model.

$GdCrO_4$ is ferromagnetic below T_C with the magnetic moments along the c axis (F_z type in Bertaut's notation) [23]. The Gd-Cr exchange interaction seems to be responsible for the increase in the Curie temperature up to $T_C = 21.3$ K, as found in the C_p data (Figs. 4 and 5). This interaction not only increases T_C but also the heat-capacity values well below T_C. With regard to the weak Gd-Cr interaction, the value $J_3/k_B = 10$ K gives a good account of the experimental $C_{p,B}$ at low temperatures (see Fig. 5) and also of ΔS_T, as discussed later (see Fig. 6). The Cr sublattice is almost saturated at $T \ll T_C$ and this interaction can be viewed as an external magnetic field of around 7 T (see Sec. V) that produces a Schottky-like anomaly or, more generally speaking, a shoulder in $C_{p,0}$ at zero field.

The polarization of the rare-earth sublattice by a weaker exchange with the $3d$ atoms was already analyzed more than 40 years ago for the distorted perovskite $NdCrO_3$ [32]. In a detailed study of $NdFeO_3$, the heat-capacity data matched very well with the result obtained for a paramagnetic Nd^{3+} in an external effective field produced by an Fe sublattice above 1 K, where Nd orders due to the much weaker Nd-Nd interaction [33]. The Fe sublattice orders at very high temperature, therefore its magnetic moment is nearly constant below 20 K and so is the effective field acting on the Nd^{3+} ions. As a result, the heat capacity agrees very precisely with the polarization model in an external field [33]. Nevertheless, these perovskites are antiferromagnetic and the staggered effective field does not help the external field in the polarization of the rare-earth ions. Moreover, Nd^{3+} is not a good ion to produce a high magnetocaloric effect because of its low magnetic moment. Moreover, its relatively large anisotropy splits the ground free atom manifold in five Kramers doublets and, at low temperature, Nd^{3+} behaves as a spin 1/2. The behavior of $GdCrO_4$ is much more favorable for magnetic refrigeration. The Gd-Cr interaction is weaker but comparable to the Cr-Cr one, consequently, the moments of the Cr and Gd sublattices grow below T_C, but at a different rate.

A simple mean-field model can be applied in order to have a qualitative explanation of the experimental results. In any case, we cannot expect a precise quantitative agreement from this model. Considering two inequivalent magnetic atoms A and B with spins s_1 and s_2, the Hamiltonian for 1 mol of the entire lattice is given by

$$H = -N_A\left[\tfrac{1}{2}z_1 J_1 \langle s_1\rangle^2 + \tfrac{1}{2}z_2 J_2 \langle s_2\rangle^2 + z_3 J_3 \langle s_1\rangle\langle s_2\rangle\right], \quad (3)$$

where N_A is the Avogadro constant, z_1 is the number of nearest A neighbors of a given A atom, z_2 is similar to z_1 for B atoms, and z_3 is the number of nearest B atoms to a given A atom. J_1, J_2, and J_3 are the exchange constants between A-A, B-B, and A-B pairs, and $\langle s_i\rangle$ the thermal and quantum average of the corresponding spins. For $GdCrO_4$, we have $z_1 = z_2 = 4$, $z_3 = 2$. The equivalent exchange field acting on Gd (see Sec. V) is $B_{ex} = z_3 J_3 \langle s_1\rangle/(g\mu_B)$, with μ_B the Bohr magneton. Results for the magnetic heat capacity C_m are plotted in Fig. 5, discarding the Gd-Gd interaction, with A = Cr, B = Gd, $J_1/k_B = 25$ K, $J_2/k_B = 0$, and $J_3/k_B = 10$ K.

Due to the Gd-Cr interaction, the peak at T_C is considerably higher than for compounds with only Cr as a magnetic atom (i.e., $LuCrO_4$, Fig. 4) because, when ordered ferromagnetically, the Cr sublattice polarizes Gd. In the mean-field model the exchange field acting on the Gd moment is proportional to the moment of Cr, due to the term of the Hamiltonian containing J_3. This term is much higher than the term with J_2, which we have neglected and in any case is zero for an antiferromagnetic Gd-Gd interaction (in such a case $\langle s_2\rangle$ should be replaced by the staggered average of the x or y

component of $\langle \mathbf{s}_2 \rangle$, zero above T_N). Neglecting J_2, the terms with J_1 and J_3 contribute to the magnetic entropy of the peak. Moreover, the heat capacity does not drop sharply below T_C, but has a shoulder at lower temperatures. The mean field is an oversimplification and predicts Curie temperatures that are too high, especially in this case of few nearest neighbors. The predicted Schottky-like contribution at low temperatures is evident and agrees with the experimental data for 5 and 9 T at temperatures far from the critical point, where the mean-field approximation is more precise.

The existence of a peak at 4.8 K in $C_{p,B=0}$ indicates another ordering process due to the much weaker Gd-Gd exchange interaction, $|J_2|/k_B \simeq 0.1$ K. The magnitude of this exchange can be estimated from the data for $GdAsO_4$ and $GdVO_4$ [31]. In these isostructural compounds, Cr is replaced by a nonmagnetic atom and orders antiferromagnetically with $T_N = 1.26$ and 2.5 K, respectively. In $GdCrO_4$ the peak is much less pronounced and, consequently, the anomalous entropy of the peak at 4.8 K is much smaller since Gd is already partially ordered due to the Gd-Cr interaction. This low-temperature ordering has been described as a ferromagnetic component along the a crystal axis (F_x type in Bertaut's notation) [23]. This behavior is surprising because, in cases with nonmagnetic atoms replacing Cr (e.g., $GdVO_4$, $GdAsO_4$), the ordering takes place at similar low temperatures but in an antiferromagnetic configuration. In $GdCrO_4$, the Gd-Cr exchange interaction acts as a constant external field. The final structure would minimize the energy in a way that is analogous to the effect of a strong external field applied to an antiferromagnet in the hard direction. The field produces a spin-flop transition in the case of weak anisotropy. The final order would not be ferromagnetic F_zF_x, but canted with the x component of the Gd moment antiferromagnetically ordered, probably F_zG_x. Moreover, a ferromagnetic Gd-Gd interaction would not produce any new transition but an increase of the order parameter, that is, the spontaneous magnetization below T_C. The assumption of a F_x component below T_N was based on a neutron diffraction experiment made on a powder with a short wavelength [23]. No extra reflections were observed below 4.8 K apart from the nuclear ones, which was considered to correspond to ferromagnetic ordering. Nevertheless, the entropy content of the peak, $\Delta S_m(T_N)/R \simeq 0.2 \ll \ln 8 = 2.08$, is very small and, consequently, the x component of the Gd moment should be much lower than its total moment, surely less than $1\mu_B$, due to the strong polarization induced by the Cr sublattice above T_N. The magnetization data at weak fields do not give an idea because of the demagnetization field, but for $B = 1.5$ T (surely above the demagnetization field) give $M = 6.8\mu_B$/f.u. at 4 K, which means a difference of $1.2\mu_B$ at the Gd site, to be ordered at T_N. This small component is difficult to be observed on powder neutron diffraction, especially in a Gd sample that is a strong absorber for thermal neutrons.

C. Magnetocaloric effect

The isothermal entropy change ΔS_T has been determined in three ways: (1) from magnetization, via the Maxwell relation $(\partial S/\partial B)_T = (\partial M/\partial T)_B$, (2) from heat capacity, and (3) directly, via Eq. (1) [see Fig. 3(a)]. In this case there is no precise way to extrapolate the heat capacity to $T = 0$ to obtain the absolute entropy, which would lead to large uncertainties in the determination of ΔS_T for different fields. Instead, we used the direct determination of ΔS_T for the fields of interest, at a temperature T_0 well above T_C, where this value is small. The measured $\Delta S_{T_0}(B)$ become integration constants in the calculation of $\Delta S_T(B)$ as follows:

$$S(T,B) = S(T_0,B) + \int_{T_0}^{T} \frac{C_{p,B}dT}{T} \tag{4}$$

and $\Delta S_{T_0}(B) = S(T_0,B) - S(T_0,0)$. Then, for any other temperature,

$$\begin{aligned}\Delta S_T(B) &\equiv S(T,B) - S(T,0) \\ &= \Delta S_{T_0}(B) + \int_{T_0}^{T} \frac{(C_{p,B} - C_{p,0})dT}{T}.\end{aligned} \tag{5}$$

Proceeding in this way, the results agree very well with those directly measured in the full temperature range, which would not be the case if $C_{p,B}$ alone were used. This direct determination of $\Delta S_{T_0}(B)$ also allows one to obtain the absolute entropy at every field B when the heat-capacity data can be extrapolated to $T = 0$ only for one of these fields. The extrapolation provides the entropy at every temperature for one field, and the direct measurements of $\Delta S_{T_0}(B)$ make its calculation possible for the other fields. The extrapolation of $C_{p,9\,\mathrm{T}}(T \to 0)$ was used to obtain the absolute entropy at 9 T, as discussed in Sec. IV B.

The values deduced from field dependent magnetization measurements agree well with the results from heat capacity. Actually, the consideration of the real internal fields on each experimental sample gives a good account of the small differences in ΔS_T obtained from $M_T(B)$ and $C_{p,B}(T)$ measurements. An estimation of the demagnetizing fields for the different sample shapes explains these differences. Moreover, the small temperature increments used for the numerical integration of Eq. (2) can give some errors in the calculations from $M_T(B)$.

The adiabatic temperature increment ΔT_S [Fig. 3(b)] has been deduced in two ways: (1) from heat capacity through the entropy derived functions [Eq. (4)] and (2) in a semidirect way, using the basic equation

$$-\Delta S_T = S(T,0) - S(T,B) = \int_{T}^{T+\Delta T_S} \frac{C_{p,B}(T)dT}{T}. \tag{6}$$

Here, ΔS_T and $C_{p,B}(T)$ are experimental values, and the integral is numerically solved for every ΔS_T data to find the upper limit of the integral and, then, $\Delta T_S(T,B)$. This second method uses only the heat capacity with field and does not require one to determine any integration constant. To obtain the integration constants at different fields in the first method, a single ΔS_T measurement was used for each field at $T = 30.9$ K. Both methods gave the same results within the experimental precision.

The magnetocaloric effect is a consequence of the magnetic properties of Cr^{5+} and Gd^{3+}, and their exchange interactions. On one hand, Cr provides a relatively high T_C in comparison with compounds with a nonmagnetic atom instead of Cr. On the other hand, the isotropic Gd allows all its $2s + 1$ magnetic levels to be occupied at zero field. This fact produces high entropy values and a large magnetic moment, which is easy

to be polarized by an external field. The Gd-Cr interaction acts as an external field polarizing the Gd atom. As a result, the MCE reaches high and wide curves with maximum values $-\Delta S_{T,\max} = 18.8$ and 29.0 J/kg K, and $\Delta T_{S,\max} = 7.9$ and 12.1 K for 5 and 9 T, respectively. The MCE keeps high values in a wide temperature range between 5 and 35 K, ideal for hydrogen liquefaction. The peak values are similar to those of several conventional materials, such as $ErCo_2$ [6], but in this compound the MCE drops to very small values just below $T_C = 35$ K.

Finally, it is worth realizing that the magnetic behavior of the scheelite polymorph of $GdCrO_4$ is completely different, i.e., antiferromagnetic, with $T_N = 21$ K [17]. The Cr-O-Cr and Cr-O-Gd angles are different in the scheelite and zircon polymorths, and the sign of the superexchange interaction depends critically on this angle. The, probably, accidental coincidence of T_C (zircon) with T_N (scheelite) gives similar heat-capacity peaks at zero field but different field dependences of magnetization [17] from which we expect very different MCEs. Midya *et al.* expected to find a significantly larger MCE for these high pressure scheelite phases [14], assuming that a larger magnetization would produce a higher MCE. However, the MCE does not depend on the absolute magnetization but rather on its temperature derivative along the field change. For the compounds studied in Ref. [14], $DyCrO_4$ and $HoCrO_4$, the magnetization depends strongly on the crystal field, which is different in each phase. For $GdCrO_4$, the spin-only Gd magnetic moment is nearly the same in both phases, but the antiferromagnetism strongly hinders the MCE, since the internal field is staggered. Actually, the MCE for low fields in an antiferromagnet is inverse ($\Delta S_T > 0$) below T_N when the external field is applied in the hard direction.

V. DISCUSSION

Usually, the MCE of a ferromagnet decreases strongly below T_C, as happens for $ErCo_2$ [6]. In the zircon phase of $GdCrO_4$, the MCE reaches its maximum value $-\Delta S_T(9\text{ T}) = 29$ J/kg K near $T_C = 21.3$ K and retains high values below this temperature down to $T_N = 4.8$ K. This is an interesting feature in regard to applications in magnetic refrigeration. Assuming $J_1 \gg J_3 \gg J_2$, the Cr^{5+} sublattice orders at a higher temperature and partially polarizes the Gd^{3+} ions. Well below T_C, the moment of the Cr^{5+} ions is nearly saturated and the weaker Gd-Cr exchange acts on the Gd moments as a constant field in the z direction. The much weaker Gd-Gd exchange would order antiferromagnetically the x or y component. Actually, the lowest-temperature phase, below 4.8 K, has been described as a ferromagnetic F_zF_x, supported by weak experimental evidence (see Sec. IV B), but it is probably a canted ferromagnetic F_zG_x. Therefore, between 4.8 and 21.3 K, the Gd sublattice behaves approximately as a paramagnet in an effective constant magnetic field.

The analysis of the predictions of the mean-field model for ΔS_T is straightforward but, in the approach of $J_2/k_B = 0$, needs the numerical solution of two equations of state. In these equations the reduced average of $\langle s_1\rangle$ and $\langle s_2\rangle$ are Brillouin functions that depend on the external field and two exchange fields deduced from the Hamiltonian given in Eq. (3). For an easy modeling and understanding of the main features, and especially to give a simple rule for the search for new compounds, instead of analyzing in detail the predictions of the mean field, we will consider the even more simplified case in which a constant $\langle s_1\rangle = 1/2$ corresponds to a fully ordered Cr^{3+} ion. The mean-field predictions do not differ much from these results except for $T > T_C$, as discussed below. In this case, the total field acting on each Gd atom can be considered as the sum of two terms, the externally applied field plus the exchange field: $B = B_{app} + B_{exc}$.

The entropy of a paramagnet for low fields or high temperatures is given by [6]

$$S/R = \ln(2s+1) - \frac{CB^2}{2T^2}, \tag{7}$$

where C is the Curie constant. That is, ΔS_T of a paramagnet is proportional to the increment of B^2, $B_i^2 - B_f^2 = (B_i + B_f)(B_i - B_f) = -(B_i + B_f)\Delta B$, where $B_{i,f}$ are the effective initial and final fields. Therefore, the MCE, for a given increment of the external field, increases with the average field. But at low temperatures the MCE decreases on increasing the average field due to the saturation of the magnetic moment. In a usual ferromagnet the mean field is proportional to the magnetization and saturates very fast below T_C, even without an external field. This is the reason why the MCE drops very fast below T_C. In the present case, due to the internal molecular field, the magnetic moments of the Cr sublattice saturate quickly below T_C, but the weaker Gd-Cr interaction does not saturate the moments of the Gd^{3+} ions down to T_N, which leaves room for the additional action of the external field.

Figure 6 shows some calculations related to $GdCrO_4$, along with experimental results. The solid colored lines are the computed $-\Delta S_T$ values for a system of paramagnetic spins 7/2 (as Gd^{3+}) for a field change $\Delta B = 5$ T, starting at different initial fields B_i. These initial fields would represent the exchange field produced by the Cr sublattice. The results, $-\Delta S_T/R$, are the molar entropy variations in units of the gas constant R, which is dimensionless and independent on the concentration of the magnetic atoms. For low B_i values, the maximum $|\Delta S_T|$ occurs at very low temperatures (orange line, calculated for $B_i = 0$). On increasing B_i, the maximum decreases and occurs at higher temperatures, as shown in Fig. 6 for $B_i = 3$, 5, and 7 T. In the high-temperature range one can observe the increase in the $-\Delta S_T/R$ curves with the average field, resulting in quite lower values for a zero initial field above 15 K (orange line). In $GdCrO_4$ this entropy change experienced by the Gd^{3+} ions must be added to the corresponding change coming from the Cr^{5+} ions. This last contribution has been computed via the mean-field Bean-Rodbell model [34] for spin 1/2. In this model the free parameters are T_C and the variation of the exchange interaction with the volume. This variation is summarized by the η parameter. For $\eta = 0$ there is no dependence of T_C with volume and values of $\eta > 1$ give rise to a first-order transition. Our chosen value $\eta = 0.1$ results in a total $-\Delta S_T/R$ contribution that agrees very well with the experimental data below T_C for $\Delta B = 5$ T, with $B_i = 7$ T as the exchange field acting on the Gd^{3+} ions. This approach is not valid above T_C where the Cr sublattice is not spontaneously ordered and, consequently, its magnetization is neither constant nor saturated. The exchange field acting on

the Gd^{3+} ions is proportional to the magnetization of the Cr sublattice, which in this T range is polarized by the external field. This effect is stronger near T_C, where the susceptibility has a maximum. Above T_C, the effective initial B_i is zero, but B_f has a value which depends on the polarization of the Cr sublattice with the external field, resulting in an effective ΔB higher than the externally applied field of 5 T. Consequently, $|\Delta S_T|$ decreases with increasing T but remains much higher than the contribution of the Cr sublattice alone (dotted line in Fig. 6), and still higher than expected for the Gd sublattice with an internal constant field plus the contribution of Cr (black line in Fig. 6).

In summary, this simple mean-field model explains the qualitative behavior of $C_{p,B}$ and ΔS_T, although it does not allow to extract precise predictions. The Gd-Cr exchange is responsible for a large entropy change under the magnetic field action due to the Gd polarization below T_C. The entropy change is also large above this temperature, in a wide temperature range. This feature becomes an important improvement in the use of magnetic refrigeration for the liquefaction of gases. It suggests an interest in searching for other ferromagnets having T_C near the boiling point of the gas to be liquified and being composed of a transition metal and a rare-earth atom, with a relatively weak exchange between both sublattices. The exchange should be strong enough to produce polarization of the rare-earth atoms but not so large as to induce saturation of this sublattice.

ACKNOWLEDGMENTS

This work has been funded by the Spanish MINECO through Projects No. MAT2013-44063-R and No. MAT2013-44964-R, DGA Consolidated Group E100, and Comunidad de Madrid Project No. S2009/PPQ-1626.

[1] K. A. Gschneider, V. K. Pecharsky, and A. O. Tsokol, Rep. Prog. Phys. **68**, 1479 (2005).
[2] B. F. Yu, Q. Gao, X. Z. Meng, and Z. Chen, Int. J. Refrig. **26**, 622 (2003).
[3] G. V. Brown, J. Appl. Phys. **47**, 3673 (1976).
[4] V. K. Pecharsky and K. A. Gschneidner, Phys. Rev. Lett. **78**, 4494 (1997).
[5] S. Khmelevskyi and P. Mohn, J. Phys.: Condens. Matter **12**, 9453 (2000).
[6] A. M. Tishin and Y. I. Spichkin, *The Magnetocaloric Effect and its Applications* (IOP Publishing, Bristol, U.K., 2003).
[7] S. W. Cheong and M. Mostovoy, Nat. Mater. **6**, 13 (2007).
[8] M. Balli, B. Jandl, P. Fournier, and M. M. Gospodinov, Appl. Phys. Lett. **104**, 232402 (2014).
[9] A. Midya, N. Khan, D. Bhoi, and P. Mandal, Appl. Phys. Lett. **101**, 132415 (2012).
[10] V. Franco, J. S. Blazquez, B. Ingale, and A. Conde, Annu. Rev. Mater. Res. **42**, 305 (2012).
[11] K. Matsumoto, T. Kondo, S. Yoshioka, K. Kamiya, and T. Numazawa, J. Phys.: Conf. Ser. **150**, 012028 (2009).
[12] T. Numazawa, K. Kamiya, T. Utaki, and K. Matsumoto, Cryogenics **62**, 185 (2014).
[13] J. Park, S. Jeong, and I. Park, Cryogenics **71**, 82 (2015).
[14] A. Midya, N. Khan, D. Boi, and P. Mandal, Appl. Phys. Lett. **103**, 092402 (2013).
[15] A. Midya, N. Khan, D. Boi, and P. Mandal, J. Appl. Phys. **115**, 17E114 (2014).
[16] E. Climent Pascual, J. Romero de Paz, J. M. Gallardo Amores, and R. Sáez Puche, Solid State Sci. **9**, 574 (2007).
[17] A. J. Dos santos García, E. Climent Pascual, J. M. Gallardo Amores, M. G. Rabie, Y. Doi, J. Romero de Paz, B. Beuneu, and R. Sáez-Puche, J. Solid State Chem. **194**, 119 (2012).
[18] R. Sáez-Puche, E. Jiménez, J. Isasi, M. T. Fernández-Díaz, and J. L. García-Muñoz, J. Solid State Chem. **171**, 161 (2003).
[19] M. Rabie, Ph.D. thesis, Universidad Complutense Madrid, 2013.
[20] Y. W. Long, Q. Huang, L. X. Yang, Y. Yu, Y. X. Lv, J. W. Lynn, Y. Chen, and C. Q. Jin, J. Magn. Magn. Mater. **322**, 1912 (2010).
[21] E. Climent Pascual, J. M. Gallardo Amores, R. Sáez Puche, M. Castro, N. Taira, J. Romero de Paz, and L. C. Chapon, Phys. Rev. B **81**, 174419 (2010), and references therein.
[22] Q. Y. Dong, Y. Ma, Y. J. Ke, X. Q. Zhang, L. C. Wang, B. G. Shen, J. R. Sun, and Z. H. Cheng, Mater. Lett. **161**, 669 (2015).
[23] E. Jiménez-Melero, P. C. M. Gubbens, M. P. Steenvoorden, S. Sakarya, A. Goosens, P. Dalmas de Réotier, A. Yaouanc, J. Rodríguez-Carvajal, B. Beuneu, J. Isasi, R. Sáez-Puche, U. Zimmerman, and J. L. Martínez, J. Phys.: Condens. Matter **18**, 7893 (2006).
[24] E. Palacios, J. A. Rodríguez-Velamazán, M. Evangelisti, G. J. McIntyre, G. Lorusso, D. Visser, L. J. de Jongh, and L. A. Boatner, Phys. Rev. B **90**, 214423 (2014).
[25] G. A. Gehring, H. G. Kahle, W. Nagele, A. Simon, and W. Wuchner, Phys. Status Solidi B **74**, 297 (1976).
[26] K. Tezuka, Y. Doi, and Y. Hinatsu, J. Mater. Chem. **12**, 1189 (2002).
[27] S. Yu. Dankov, A. M. Tishin, V. K. Pecharsky, and K. A. Gschneidner, Jr., Phys. Rev. B **57**, 3478 (1998).
[28] M. Rappaz, M. M. Abraham, J. O. Ramey, and L. A. Boatner, Phys. Rev. B **23**, 1012 (1981).
[29] S. L. Chaplot, L. Pintschovius, N. Choudhury, and R. Mittal, Phys. Rev. B **73**, 094308 (2006).
[30] Y. W. Long, L. X. Yang, Y. Yu, F. Y. Li, R. C. Yu, S. Ding, Y. L. Liu, and C. Q. Jin, Phys. Rev. B **74**, 054110 (2006).
[31] J. H. Colwell, B. W. Mangum, and D. D. Thornton, Phys. Rev. B **3**, 3855 (1971).
[32] R. M. Hornreich, Y. Komet, R. Nolan, B. M. Wanklyn, and I. Yaeger, Phys. Rev. B **12**, 5094 (1975).
[33] J. Bartolomé, E. Palacios, M. D. Kuzmin, and F. Bartolomé, I. Sosnowska, R. Przenioslo, R. Sonntag, and M. M. Lukina, Phys. Rev. B **55**, 11432 (1997).
[34] C. P. Bean and D. S. Rodbell, Phys. Rev. **126**, 104 (1962).